**Proceedings of the ASME 2024**
**International Design Engineering Technical Conferences and**
**Computers and Information in Engineering Conference**
**IDETC/CIE2024**
**August 25-28, 2024, Washington, DC**

# IDETC2024-146330

# MULTILEVEL DECISION SUPPORT FRAMEWORK FOR THE SIMULTANEOUS DESIGN EXPLORATION OF MATERIAL STRUCTURES AND PROCESSES

**H M Dilshad Alam Digonta**
Doctoral Student
Systems Realization Laboratory @ FIT
Florida Institute of Technology,
Melbourne, FL, USA

**Anand Balu Nellippallil**[1]
Assistant Professor
Systems Realization Laboratory @ FIT
Florida Institute of Technology,
Melbourne, FL, USA

**Mathew Baby**
Doctoral Candidate
Systems Realization Laboratory @ FIT
Florida Institute of Technology,
Melbourne, FL, USA

## ABSTRACT

*Traditional manufacturing, such as steel manufacturing, involves a series of processes to realize the final product. The properties and performance of the final product depend on the material processing history and the microstructure generated at each of the processes. Realizing target product performance requires the simultaneous design exploration of the material microstructure and processing, taking into account the multilevel interactions between the material, product, and manufacturing processes. This demands the capability to co-design, which involves sharing a ranged set of solutions through design exploration across multilevel and providing design decision support.*

*In this paper, we present a co-design exploration framework for multilevel decision support. Using the framework, we model the interactions and couplings between the levels and facilitate simultaneous decision-based design exploration. The framework integrates the coupled compromise Decision Support Problem (c-cDSP) construct with interpretable Self-Organizing Maps (iSOM) to facilitate (i) the formulation of the multilevel decision support problems taking into account the interactions and couplings between levels, (ii) the simultaneous visualization and exploration of the multilevel design spaces, and (iii) decision-making across levels for multilevel designers. The efficacy of the framework is tested using a hot rod rolling problem focusing on the interactions between the dynamic and metadynamic phases of material recrystallization and the thermo-mechanical processing during the hot rolling process. The framework is generic and supports the co-design exploration of systems characterized by multilevel interactions, couplings, and multidisciplinary designers.*

***Keywords***: Co-design, multilevel decision support, coupled-compromise Decision Support Problem (c-cDSP), interpretable Self-Organizing Maps (iSOM)

## 1. FRAME OF REFERENCE

Traditional manufacturing processes, such as steel manufacturing, involve a sequence of processes to realize the final product. The design of such systems needs to consider the information flow and interactions between the disciplines of material, product, and manufacturing processes. Designers are required to consider the interrelated variables, the conflicting goals and constraints, and the interactions and couplings between these different disciplines, making the design of these systems complex. Due to this, coming up with comprehensive system-wide satisfying solutions that take into account the information flows, process interrelations, conflicting goals, and couplings between the disciplines is a challenge. One approach to managing the design complexity is to decompose the system-level problem into a set of interdependent and distributed subsystem-level problems, where the multiple levels correspond to the different disciplines of material, product, and manufacturing process. The multiple design levels are characterized by the respective multidisciplinary designers, such as manufacturing process, materials, and product designers, who are equipped with domain-specific tools and knowledge to formulate the distributed design problems specific to their discipline. Such a multilevel design approach focuses on coordinating the couplings between the levels and finding solutions that satisfy the designers' requirements at the individual levels of the multiple design levels. Multidisciplinary design optimization (MDO) approaches [1-4] are used to address such problems. The focus in MDO approaches is to identify single-point design solutions via extensive optimization methods and

[1] Corresponding author, Email: anellippallil@fit.edu

detailed analysis models for each of the disciplines. The MDO approaches also require compliance with a formal design framework, which often entails substantial iteration within and between the design levels. In the early stages of design, when the designer's focus is on quickly finding a satisfying region of the design space for the multiple design levels, these characteristics of the optimization approaches create a challenge [5]. Therefore, we need approaches that facilitate the simultaneous design exploration of complex design spaces across multiple levels and efficient identification of satisfactory solution regions for decision-making. This involves facilitating '**co-design exploration**', that is, *the capability of distributed designers or decision makers (material, product, and manufacturing process designers, respectively) at multilevel to collaboratively share their information, knowledge, and resources in an integrated fashion to achieve the simultaneous design exploration of the material, product, and associated manufacturing processes*.

The properties and performance of a product are defined by the material processing history and the microstructure generated at each of the processes. An example is the hot rod rolling process of steel, where the properties of the semi-product rod are defined by the microstructure developed at various stages of the hot rolling process and the associated thermo-mechanical processing history during the reheating, rolling, and cooling stages. Due to the relations existing between the material processing history, microstructure generated, and the product property and performance, achieving targeted product performance requires considering the design of the overall system, which includes the co-design exploration of the product, material, and manufacturing process systems, and their interrelations and couplings [6].

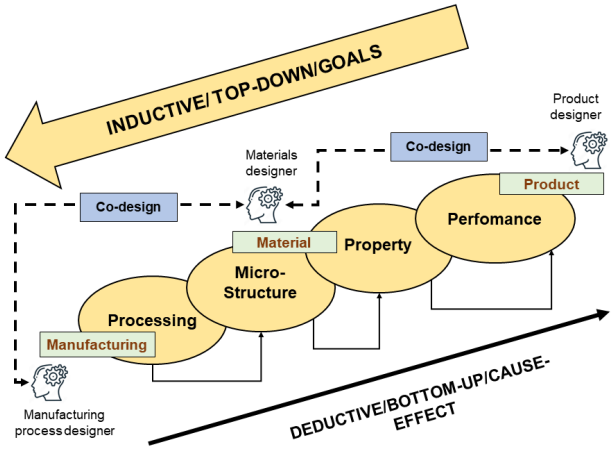


**FIGURE 1:** Olson's PSPP relations and co-design between manufacturing process, material, and product

An integrated, top-down, systems-based approach is needed to co-design these multilevel systems, starting with the performance required for the product and then inversely designing the levels of material microstructures and thermo-mechanical processing history to realize the target performance. Olson's **P**rocessing-micro**S**tructure-**P**roperty-**P**erformance (PSPP) relations [7] establish the basis for the inverse, systems-based co-design exploration by linking the disciplines of product, materials, and manufacturing processes, as shown in Figure 1. According to the PSPP relations, the manufacturing processing history determines the material microstructure and properties, which determines the product properties and performance. The Integrated Computational Materials Engineering (ICME) effort offers guidance for the simulation-supported design of material, product, and manufacturing process systems. ICME emphasizes using simulation-based design to realize products and materials concurrently in a top-down fashion using the PSPP relations generated through integrated material and process models across various lengths and time scales. By utilizing simulation-supported systems design approaches, designers are able to comprehend the complex relationships in materials design better and make well-informed design decisions [8]. Materials design for ICME is essentially viewed as a decision-making process using simulation-based design. However, simulation models used in materials design are typically incomplete, inaccurate, and not of equal fidelity. They are abstractions of the real physical material phenomena [9] and embody uncertainty. Single-point solutions based on optimization are sensitive to uncertainty and do not hold when conditions change. Therefore, the multilevel design necessitates exploring the solution spaces and identifying solution regions, rather than single-point solutions, that satisfy and suffice the designer's requirements across multiple levels and are relatively insensitive to uncertainties. Such solution regions are defined as "*satisficing solutions*" [10].

From a systems design perspective, we view design as a top-down, goal-oriented, decision-based process supported by simulations [11, 12]. We advocate the Decision-Based Design (DBD) paradigm advocated by Mistree and co-authors [13]. In DBD, design problems are modeled as Decision Support Problems (DSP) using Decision Support Problem Techniques (DSPT) and constructs, see [14, 15]. The DSP technique is based on the notion of bounded rationality proposed by Herbert Simon [16]. In DBD, decisions are made using information generated from simulation models. The compromise Decision Support Problem (cDSP) [17] construct is used to formulate and solve design problems involving many conflicting goals and seek satisficing solutions through design exploration and trade-off.

Several recent works address the inverse design of material structures from a top-down systems perspective. A framework presented by Adams and co-authors [18] addresses the inverse relations between the material microstructure, properties, and processing path and uses spectral representations to establish the invertible linkages. Kalidindi and co-authors [19, 20] present a materials knowledge system approach that facilitates the flow of high-fidelity information in both directions between the constituent length scales, offering a new technique for concurrent multiscale modeling, supporting inverse design. A probabilistic inverse design machine learning framework is presented by Ghosh and co-authors [21] to carry out explicit inverse design using conditional invertible neural networks. A deep reinforcement learning (DRL) scheme is presented by Sui and co-authors [22] to automate the inverse design of composite

material structures for realizing target performance. Kim and co-authors [23] introduce an Artificial Neural Network (ANN) based design method to achieve specific user-defined features through an inverse design approach for zeolites. Chen and co-authors [24] introduce a generative deep neural network that utilizes inverse design, backpropagation, and active learning to support the design of composite materials. A machine learning-based inverse design technique is also presented by Kumar and co-authors [25] to design the topology of metamaterials with tailored properties. All these approaches use advanced machine learning and data-driven techniques to help establish invertible linkages for material design using the PSPP relations that can be further used in engineering design for decision-making. These approaches are focused on problems where the structure-property relations can be inverted in some manner.

Even though there are advanced materials modeling techniques to establish inverse relations, it is noticed that the decision-making for materials design using engineering design techniques is mostly sequential. In the current techniques, the design spaces for the different disciplines, namely product design, materials design, and manufacturing process design, are formulated and solved sequentially without taking into consideration the complex interactions and couplings between the different disciplines. The sequential, discipline-specific design process results in decisions at one level/discipline that can cause unintended consequences to other levels/disciplines since the interactions are not captured and decisions are not made simultaneously [26, 27]. Therefore, the independent decisions across individual levels fail to consider the multilevel interactions and could cause design conflicts, impacting the overall system performance.

Multidisciplinary design optimization (MDO) approaches such as bi-level integrated system synthesis (BLISS) [1, 2], collaborative optimization (CO) [3], and analytical target cascading (ATC) [4] are discussed in the literature to address the optimization of the multilevel system while considering the interactions across the multiple levels. Martins and Lambe [28] describe that the overall system performance is influenced by individual-level performance and their interactions, which serves as the primary motivation for MDO. MDO problem formulations focus on optimizing the entire system rather than individual levels or subsystems sequentially [27]. In MDO, subsystems are formulated by combining data generated from multi-fidelity models [29], such as empirical models for manufacturing processes, physics-based material models, and data-driven surrogate models that are abstractions of the physical phenomena for a defined design space [9]. These models are used to establish quantitative links and interrelations between the individual levels/disciplines in MDO. Ituarte and co-authors use MDO with surrogate models [27] to establish a computer-aided expert system that couples the design exploration and trade-off of product, material, and manufacturing process designs for digital manufacturing.

However, these MDO approaches employ rigorous and iterative optimization techniques involving extensive optimization loops within and between levels to identify unique single-point solutions. As discussed above, when designers are focused on design exploration in the early stages of design and interested in quickly identifying satisfactory regions of interest, such intensive MDO approaches are not appropriate. Addressing the challenges of MDO for early-stage design exploration, satisficing design strategies are proposed.

Multilevel approaches that support identifying satisficing design solutions are discussed in the literature. The Inductive Design Exploration Method (IDEM) is proposed by Choi and co-authors [30] to support the design of multilevel systems. Using IDEM, robust ranges of satisficing solutions are identified and sequentially mapped across the multilevel in an inverse manner. IDEM, however, has restrictions in the number of design variables and responses that can be considered, errors due to discretization, increased computational expense for improved accuracy, and limited design flexibility due to sequential mapping of design spaces [31]. Nellippallil and co-authors [32] present the Goal-oriented Inverse Design (GoID) method that addresses some of the limitations of IDEM. GoID method supports the design of multilevel systems through compromise decision support problem (cDSP)-based sequential design exploration. Using GoID, robust satisficing solutions are identified and propagated sequentially across levels as goal targets for the DSP in an inverse manner. Both IDEM and GoID methods are sequential in nature, with a focus on realizing the goals and satisfying the constraints of the individual discipline/level at a time. These methods do not address the coupled interactions, the management of design conflicts between levels, and the simultaneous exploration of the multilevel design spaces for decision-making. Recent works address some of the above-mentioned limitations. Sharma and co-authors [33, 34] showcase the utility of coupled cDSP (c-cDSP) for modeling problems with different forms of coupled interactions between levels. Further, Baby and Nellippallil [35] present an information-decision framework to detect and manage design conflicts in a systematic manner for multilevel problems. However, the above-discussed approaches do not address the simultaneous design exploration of the multilevel for decision-making. In a recent work, Baby and co-authors [36] present a Co-Design Exploration of Multilevel systems under Uncertainty (CoDE-MU) framework to support the co-design exploration of multilevel design spaces and identify satisficing solutions that are common within and between the levels. The CoDE-MU framework as presented by Baby and co-authors, did not address coupled interrelations between levels.

In this paper, we use the CoDE-MU framework for the simultaneous co-design exploration of material microstructures and processing levels, given the coupled interrelations between the levels. The CoDE-MU framework facilitates (i) modeling the level-specific information flow and the interactions between levels of the disciplines (material processing and material microstructure) and (ii) simultaneous exploration of the multilevel solution spaces to identify common satisficing design solutions for all the disciplines. The coupled-cDSP construct is used in the framework to formulate the multilevel problem. The objective function of c-cDSP involves a combination of

preemptive and Archimedean formulations. By combining the two formulations, designers are able to account for many conflicting goals (more than three goals) within a single design level and consider the couplings and interrelations between multiple design levels. In this paper, we propose consistency constraints in the coupled cDSP formulation to model the couplings between the levels/disciplines. These constraints ensure the consistency of coupled variables shared between levels. The simultaneous visualization and exploration of the many goals within and between design levels is facilitated by the integration of interpretable Self-Organizing Maps (iSOM) in the framework [37]. iSOM facilitates the co-design exploration by allowing the designer to simultaneously visualize the high-dimensional solutions spaces in two dimensions and easily navigate the multilevel design spaces to identify common satisficing solution regions, thus facilitating decision support. The efficacy of the multilevel decision support framework is tested using a hot rod rolling problem focusing on the interactions between the dynamic and metadynamic phases of material recrystallization and the thermo-mechanical processing during the hot rolling process. The sections of the paper are discussed below.

In Section 2, we describe the hot rod rolling problem and the design approach used to formulate the multilevel hot rod rolling problem. In Section 3, we discuss the multilevel decision support framework for simultaneous co-design exploration. In Section 4, we showcase the efficacy of the framework in the simultaneous multilevel co-design exploration and decision support using the hot rod rolling problem. We close the paper by summarizing the key functionalities and with our remarks in Section 5.

## 2. PROBLEM DESCRIPTION

### 2.1 Co-design of hot rod rolling process chain and steel microstructures

Steel manufacturing involves a sequence of manufacturing processes. The hot rolling process is a major manufacturing process in the steel manufacturing process for producing semi-products like rods and sheets. Hot rolling is generally used to obtain fine grains of austenite through the thermo-mechanical hot deformation process. The fine grains of austenite help achieve fine grains of ferrite through phase transformation during the cooling process that follows rolling. The formation of the fine grains of ferrite supports the achievement of improved mechanical properties in the hot-rolled product. From a design perspective, our interest in this problem lies in co-designing the steel manufacturing process chain, involving hot rolling and cooling processes, with the steel microstructures.

One of the requirements identified in the problem is to achieve a target final austenite grain size (AGS) after the hot rolling process. To achieve a target final AGS, several microstructural phenomena during rod rolling need to be considered, which include dynamic recovery, dynamic recrystallization, metadynamic recrystallization, static recovery, static recrystallization, and grain growth after recrystallization [38]. It is understood that static recrystallization plays a major role in plate rolling. However, for the hot rod rolling process, dynamic recrystallization plays a major softening role for the microstructures due to the higher strain rates and shorter interpass time involved with the rod rolling process [39]. The dynamic recrystallization phenomenon is followed by metadynamic recrystallization, which removes the dynamically recrystallized microstructure. It is identified that metadynamic recrystallization kinetics is highly dependent on strain rate and is weakly dependent on the deformation temperature [39]. The high strain rate sensitivity of metadynamic recrystallization plays a major role in defining the final austenite grain size and the recrystallization kinetics. Following complete metadynamic recrystallization, the coarsening of the equiaxed austenite grains happens through the grain growth phenomenon. The grain size after grain growth defines the microstructure of the steel after hot rod rolling. The conditions of the final steel microstructure are defined by the effects of the interrelationships and couplings involved in the above-discussed microstructural and material processing phenomena.

From an engineering design perspective, there needs to be a fundamental understanding of the interdependent nature of the multilevel materials, manufacturing process, product design decisions, and the couplings between product, material, and manufacturing process levels. Towards this, in this paper, we study the co-design of the hot rod rolling process of steel and the hot rolled rod microstructures after dynamic and metadynamic recrystallizations. We consider the hot rolling process chain (multiple stages) as one manufacturing process and the dynamic, metadynamic recrystallizations and grain growth as different material microstructure phases to realize the rod (product). To frame the design problem, we assume that dynamic recrystallization occurs first and metadynamic recrystallization follows complete dynamic recrystallization. Since our interest is in inverse top-down design, we start with the requirements of the product and map these requirements to the material microstructure and material processing during the manufacturing process. For the hot rod rolling problem, the austenite grain sizes and recrystallization kinetics after metadynamic recrystallization and grain growth are considered as the end requirements and will be considered in design level 1 to facilitate inverse co-design. These requirements depend on the microstructure factors after dynamic recrystallization and material processing variables during rolling. The dynamic recrystallized grain size and recrystallization kinetics requirements are considered in design level 2 in an inverse manner. These requirements depend on the coupled information from design level 1, the microstructure information before rolling, and the material processing variables during rolling. More details on the problem are discussed in Section 4. To address the co-design problem, decisions need to be made by coordinating and investigating the interactions among the product designer (for the rod), materials designer (for the microstructure), and manufacturing process designer (for material processing), using computational process-structure-property-performance models for hot rod rolling.

### 2.2 Multilevel co-design exploration approach in the context of the problem

In Figure 2, we show a generic schematic of the co-design exploration approach for problems involving product, material, and manufacturing processes and their interactions. The approach involves establishing a forward processing-structure-property-performance (PSPP) workflow for the problem. For the hot rod rolling problem, we focus on the hot deformation of the material during rolling, the recrystallization of austenite grains during dynamic recrystallization, and the recrystallization of austenite grains during metadynamic recrystallization and grain growth. The forward PSPP workflow is established using well-established integrated mathematical models from the literature for the hot rolling process and microstructure evolution; see details in Appendix A. Once the PSPP linkages are established, a model-based information workflow is developed to capture the interrelation and couplings between the manufacturing process, material, and product; see Figure 2. We discuss this in detail in Section 3. We begin the multilevel co-design process once the forward information workflow is generated. The decision-based co-design exploration of the manufacturing process chain is carried out starting from the end product requirements. Co-design between distributed designers is facilitated through shared solution spaces of a coupled multilevel decision support problem with the capability to explore, evaluate, and modify ranged sets of design specifications across multilevel. Specifically, a coupled compromise Decision Support Problem is used to formulate the multilevel goals and requirements. Using the c-cDSP, the interactions between the different disciplines are captured, and satisficing solutions regions across the coupled design spaces are sought through co-design exploration. Design Level '1' is defined by formulating a multi-objective product-level design problem to achieve the mechanical property goals of the product. The microstructure variables from the materials discipline serve as the input variables for the product decision support problem. Design Level '2' is defined at the material level by considering the multiple microstructure requirements. The processing variables from the manufacturing discipline serve as input for the materials problem. Design Level '3' considers the requirements from the manufacturing process level given the coupled information from the material microstructure and product.

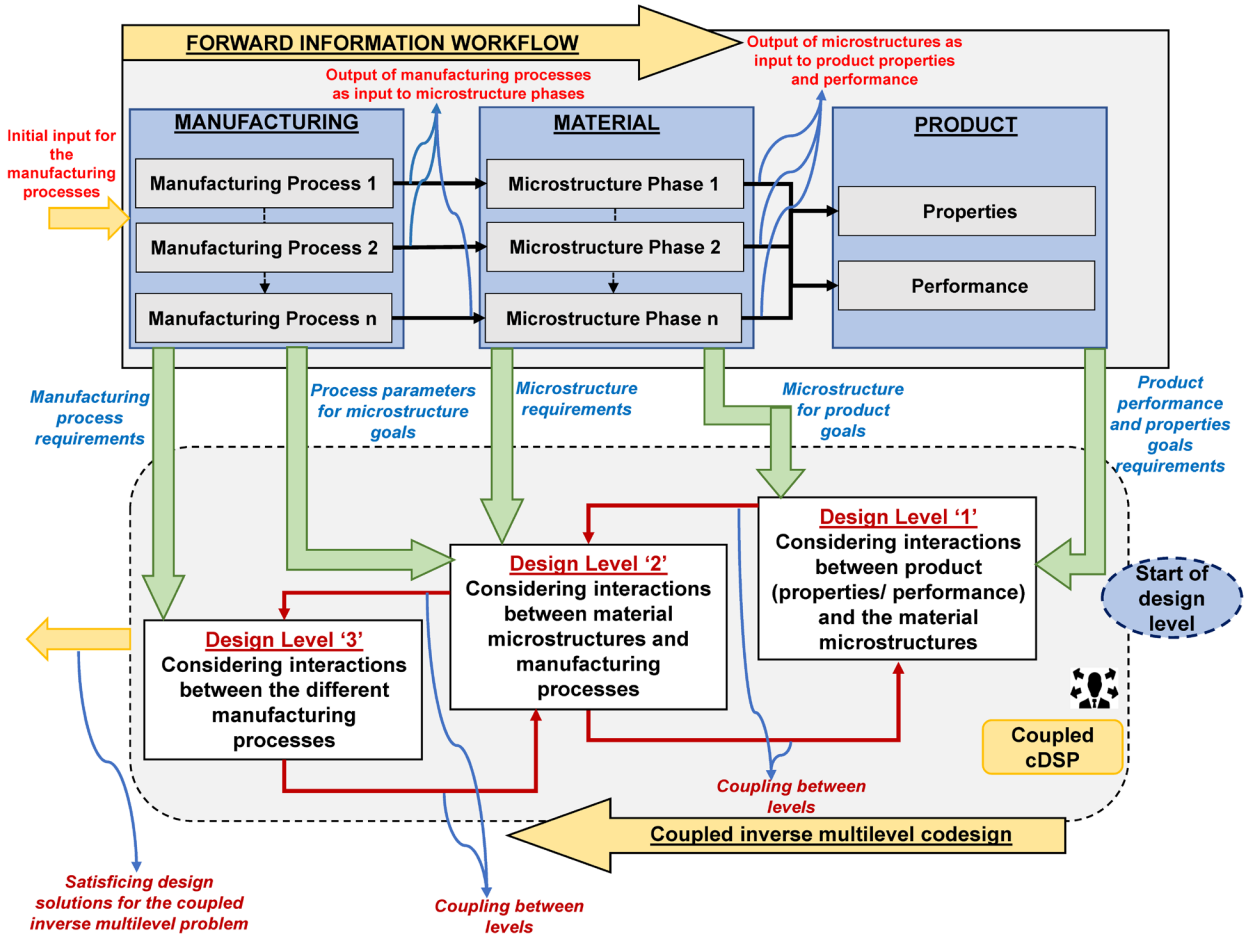


**FIGURE 2:** Forward information workflow and the inverse coupled design for the multilevel problem involving manufacturing process, material, and product.

As discussed in Section 1, sequential decision-making of the levels in an isolated manner will result in design conflicts. Design conflicts will result in reduced overall system performance. Therefore, it is essential to co-design the multiple levels considering their interactions and couplings. In this paper, we present a co-design exploration framework for multilevel decision support. Using the framework, we model the interactions and couplings between the levels and facilitate simultaneous decision-based design exploration. The framework integrates the coupled compromise Decision Support Problem (c-cDSP) construct with interpretable Self-Organizing Maps (iSOM) to facilitate (i) the formulation of the multilevel decision support problems taking into account the interactions and couplings between levels, (ii) the simultaneous visualization and exploration of the multilevel design spaces, and (iii) decision-making across levels for multilevel designers. We discuss the multilevel decision support framework in the next section.

## 3. MULTILEVEL DECISION SUPPORT FRAMEWORK FOR THE SIMULTANEOUS DESIGN EXPLORATION OF MATERIAL STRUCTURES AND PROCESSES

In this section, we present a multilevel decision support framework for the simultaneous design exploration of material structures and processes. The framework facilitates the decision-based simultaneous design exploration of multilevel. The framework is modified from the Co-Design Exploration of Multilevel systems under Uncertainty (CoDE-MU) framework presented by Baby and Co-authors [36]. We discuss the design constructs used in the framework below.

### 3.1 Construct and tools used in the framework

The primary constructs used in the framework are: (i) the coupled cDSP (c-cDSP) construct and (ii) the iSOM visualization tool.

#### 3.1.1 The coupled cDSP (c-cDSP) construct

The coupled cDSP [34] is a decision support problem (DSP) construct that supports designers in modeling multiple goals within and between multiple levels. The coupled cDSP construct is used to model the relationships and consider the decisions across various design levels/disciplines. The decisions made at individual levels are focused on achieving the multiple goals within the levels through trade-offs. We capture the level-specific information in a c-cDSP using the keywords - *Given, Find,* and *Satisfy* of a c-cDSP formulation. The information pertains to the design variables, goals, and constraints specific to the level. The primary focus of using the c-cDSP is to identify solutions that *minimize* the total deviation of all the design goals in the system from their target values, referred to as the '*deviation function*.' The deviation function in c-cDSP is modeled using a combination of preemptive and Archimedean formulations. A preemptive formulation is used to capture the relations among the multiple levels of a decision hierarchy. Design goals at multiple design levels are categorized into different ordered sets in the preemptive formulation. The order of the sets defines their priority. The design level 1 is given higher priority and defined first in the set, followed by the rest of the levels in their order of priority. In c-cDSP, design goals at the higher priority set are realized first before goals at subsequently lower levels [17]. The Archimedean formulation allows the consideration of multiple goals at the design level. The multiple goals at a level are considered by assigning different weight preferences. The weights are values between 0 and 1 (summing up to 1) and signify differences in preferences amongst the goals at a level. By combining the Preemptive and Archimedean formulations, designers are able to formulate the multilevel problem with multiple goals at each level. Designers use the Archimedean formulation at the individual levels to address the many design goals that require trade-offs. The Archimedean formulation works by assigning weight to goals in a priority set to account for the goal's relative priority at the level. A higher weight value to a goal indicates more importance for that goal at a specific level compared to others. The Decision Support in the Design of Engineering Systems (DSIDES) platform is used to formulate and execute the coupled-cDSP.

#### 3.1.2 iSOM tool for visualization and co-design exploration

interpretable Self Organizing Map (iSOM) [40] is a machine-learning-based visualization tool that helps to efficiently visualize high-dimensional data using two-dimensional (2D) plots. Specifically, it is a modified form of the artificial neural network algorithm developed by Kohonen [41] - conventional Self-Organizing Map (SOM) [42]. The modifications to SOM help avoid self-intersection, making the iSOM plot interpretable. iSOM is a scalable visualization tool that can be used to visualize any number of dimensions as presented by Sushil and co-authors [37]. The advantages of iSOM in terms of being easily scalable and interpretable make it an ideal choice to facilitate design space exploration in real-world problems. In the framework, we used iSOM to visualize the solution space of our decision support problem across multiple levels to support co-design. The iSOM tool is available in the form of a MATLAB code [40].

### 3.2 Decision support using the framework

The structure of the framework is described in detail in this section. The framework is comprised of four blocks - Blocks A, B, C, and D. The framework and its blocks are depicted in Figure 3. A detailed description of each block follows.

*Block A:* Design problem and level-specific information collection.

In Block A, the designer gathers information regarding the multilevel design problem, its levels, and their relations using the following steps – Steps A1 to A3.

*Step A1*: The designer begins by identifying the different levels of the decision hierarchy in the problem.

*Step A2*: The designer then proceeds to collect information specific to the decisions at each level identified in Step A1. The level-specific information collected includes (i) design variables and bounds, (ii) design goals and targets, (iii) models relating the variables and goals, and (iv) level constraints.

*Step A3*: Based on the level-specific information gathered in Step A2, the designer established the relations between the levels

in terms of the flow of information. The flow of information between levels includes i) shared design variables and ii) propagated values of design variables and other parameters. At the lower level of the decision hierarchy, copies of shared design variables are used as level-specific design variables. A consistency constraint ensures that the shared design variable at the lower level stays consistent with the upper level.

*Block B:* Modeling decision support problems across multiple levels and their interactions.

Using the information from Block A, in Block B, the decision problems across multiple levels and their interactions are modeled as a c-cDSP by the designer. This step, Step B1, is detailed below.

*Step B1*: The multilevel decision problems and interactions across levels are modeled using the c-cDSP construct. In the c-cDSP, separate instances of the c-DSP construct are used to model decision problems at the individual levels. The *Given*, *Find*, and *Satisfy* keywords of the cDSP constructs help capture level-specific information. The interactions among the cDSPs for each level are modeled using the shared design variables and other propagated information connecting the levels, as determined in Step A3. The deviation function of the c-cDSP is modeled using a combination of Preemptive and Archimedean formulations. Decisions in manufacturing process systems are made hierarchically across multiple levels. For a design problem with two design levels, decisions at Design Level 1, which are made first, take higher priority. This is followed by decisions at Design Level 2 being given lower priority. We use the preemptive formulation to assign different priority levels to the design goals at Levels 1 and 2. At a level, the difference in preferences among the many conflicting design goals is modeled using the Archimedean formulation. In the Archimedean formulation, different weights are assigned to the various goals. The weights assigned are values between 0 and 1 (summing up to 1), with higher values indicating higher preference. By combining the Preemptive and Archimedean formulations in the c-cDSP, designers can consider many design goals requiring trade-offs at each level and relations across levels of a multilevel decision problem. A detailed explanation of the c-cDSP is provided in the following section, Section 4. DSIDES platform is used to formulate the c-cDSP.

*Block C:* Generation of multilevel design solutions

In Block C, the c-cDSP formulation created in Block B is executed for different multilevel design scenarios to generate different multilevel design solutions. Block C is implemented in two steps.

*Step C1*: We create different multilevel design scenarios to execute the c-cDSP in this step. Sample multilevel design scenarios are depicted in Step C1 of Block C, Figure 3. A multilevel design scenario is created by combining individual-level design scenarios for Design Levels 1 and 2, which are created using Latin hypercube sampling in all possible combinations. In each individual-level design scenario, different weights (values between 0 and 1 that add up to 1) are assigned to the design goals at the level. The weights indicate the difference in preferences amongst the goals, with higher values indicating higher preference. If there are 'n' unique design scenarios at an individual level and 'm' levels, there exist $n^m$ distinct multilevel design scenarios. In this paper, $n^2$ multilevel design scenarios are considered for the two-level problem.

*Step C2*: We execute the formulated c-cDSP in the DSIDES platform for each of the $n^m$ multilevel design scenarios to generate design solutions across the levels.

*Block D:* Visualization and co-design exploration.

In this block, we use the iSOM plots to visualize the solution spaces at individual levels. We then perform a co-design exploration of the solution spaces to find a common satisficing solution for the goals across the levels. Block D is executed in two steps, as detailed below.

*Step D1*: In this step, we train the iSOM algorithm with the weights assigned to the goals in each design scenario and the corresponding values for the goals at multiple levels. The trained iSOM generates 2D plots for each input weight and output goal across multiple levels. Designers use the iSOM plots of the output goals to carry out co-design exploration in Step D2.

*Step D2*: The iSOM plots for the goals are explored in this step to determine common satisficing solution regions for the goals across multiple levels. The designer begins by setting satisficing limits for the individual goals to identify satisficing design regions for each goal. The dots on the grid represent the design scenarios associated with those specific grid points. The dot's size corresponds to the number of design scenarios mapped to the specific iSOM grid point. Hexagonal grid points with red borders in the individual output iSOM plots indicate the satisficing solutions regions for each goal; see Step D2 of Block D in Figure 3. Using the initial satisficing solution regions of the individual goals, the designer carries out co-design exploration to identify common satisficing solutions for all the goals across the levels.

A systematic approach is used to carry out the co-design exploration. Systematic co-design exploration requires three steps.

*Step 1*: Determination of whether relaxation of the satisficing goal limit is required.

To determine this, the designer needs to ask, "Is there a common region in the satisficing solution for all the goals across the levels?"

- If the answer is "No," the designer proceeds to Step 2.
- If the answer is "Yes," the co-design exploration is complete. The designer has identified a common satisficing solution for all the goals across the levels.

*Step 2*: Identify the goal to be excluded from the satisficing limit relaxation.

The designer identifies a goal across the different levels whose satisficing goals cannot be relaxed due to the formulation of the problem. This goal is a critical goal that the designer identifies. All the remaining goals are collectively called the non-excluded goals.

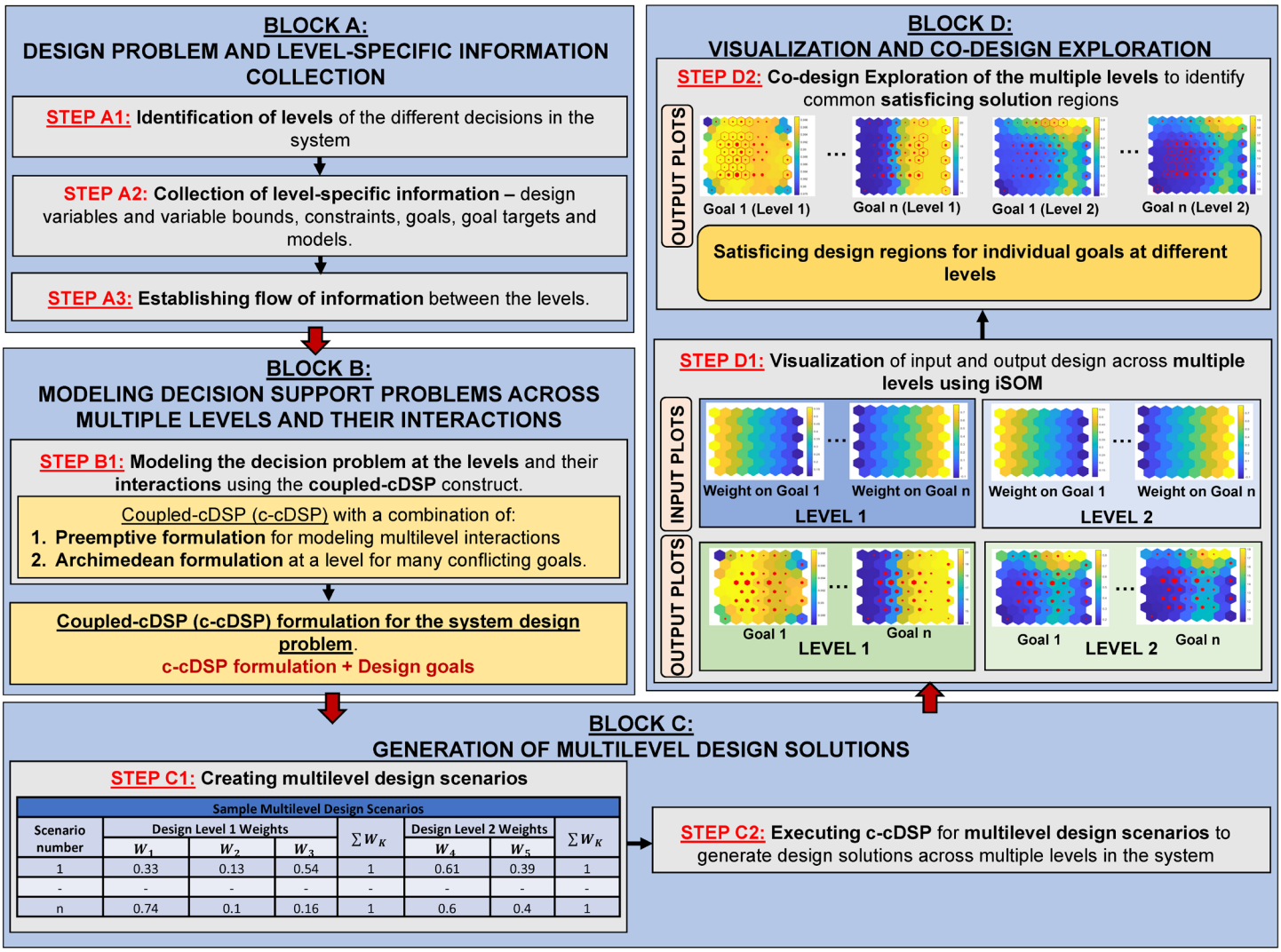


**FIGURE 3:** Multilevel decision support framework [36]

*Step 3*: Relaxation of satisficing limit for the non-excluded goals.

- Based on the designer's judgment, a goal from the non-excluded region is selected.
- The designer then looks for any common iSOM grid points in the satisficing solution region between the chosen and excluded goals.

After the end of Step 3, the designer identifies common satisficing solution regions for all goals across the multiple levels. The designer determines the design scenarios mapped to those regions using the identified common regions. From the design scenarios, the designer then identifies the corresponding design variables and goal values for the satisficing design solutions. The designer can also understand the effect of weight on different goals and the change of variable values on the goals across multiple levels by analyzing the iSOM input and output plots.

This framework is generic in nature. Designers are able to use the framework to formulate design problems that include interactions between multiple levels and many conflicting goals at individual levels and carry out co-design exploration. In the next section, we demonstrate the efficacy of the framework in supporting the co-design of multilevel systems using a hot rod rolling problem.

## 4. EXAMPLE PROBLEM: MULTILEVEL CO-DESIGN EXPLORATION OF HOT ROD ROLLING PROCESS CHAIN AND MICROSTRUCTURE

The efficacy of the proposed multilevel decision support framework is tested using the hot rod rolling problem, focusing on the co-design of the material microstructure and the hot rolling process chain. In Figure 4, we show the hot rolling process and the microstructural information at different time and space points of the manufacturing process and material/product, respectively. The steel manufacturing process chain involves the hot rod rolling process and cooling of the rod. In hot rod rolling,

a preheated billet from a casting unit is passed through a set of rollers. The steel billet is thermo-mechanically deformed as it passes through the rollers. The high strain rate and high-temperature process results in the evolution of the microstructure of steel. Two major microstructure evolution phenomena, namely, dynamic recrystallization and metadynamic recrystallization, occur during the rolling process.

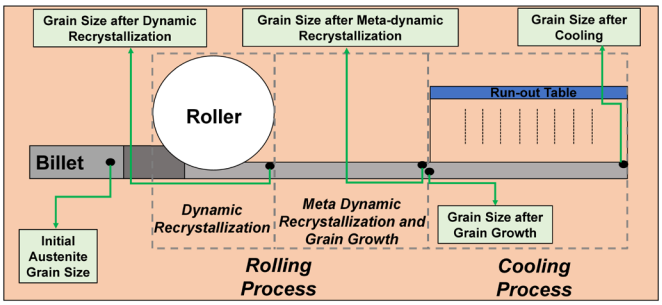


**FIGURE 4:** Schematic showing the hot rod rolling process chain and the microstructure at different stages

Recrystallization involves the formation of new grains from old grains. The dynamic recrystallization is initiated during the deformation process as the steel billet is in contact with the roller. Metadynamic recrystallization typically follows dynamic recrystallization and replaces the dynamically recrystallized grains. To formulate the design problem, we assume that dynamic and metadynamic recrystallization occur sequentially, with dynamic recrystallization occurring first and metadynamic recrystallization following it. This assumption allows us to model the information workflow of the material microstructure and helps define the decisions that need to be made, given the information flow. Grain growth occurs after recrystallization, defining the final austenite grain size after rolling. The hot rolled rod is further passed to the cooling process, where the material is cooled, and different phases of steel are obtained. Each of these sequential processes influences the microstructure of the end product. We focus on the hot rolling process problem and define the metadynamic recrystallization and grain growth stage as "Design Level 1" and the dynamic recrystallization stage as "Design Level 2."

In Figure 5, we depict the forward information workflow for the problem connecting the manufacturing process and the material structure. The multilevel inverse co-design is shown using the two design levels defined. In the forward flow of information, we see that the information from the manufacturing process chain defines the material microstructure. Dynamic and metadynamic recrystallization are considered sequentially as microstructure phases 1 and 2, respectively. Manufacturing process variables, namely strain rate ($\dot{\varepsilon}_d$), temperature ($T_d$), and strain ($\varepsilon$), and material microstructure variable, namely initial austenite grain (AGS), determine the dynamic grain size ($D_{dync}$) and grain fraction ($X_{dyn}$) during dynamic recrystallization.

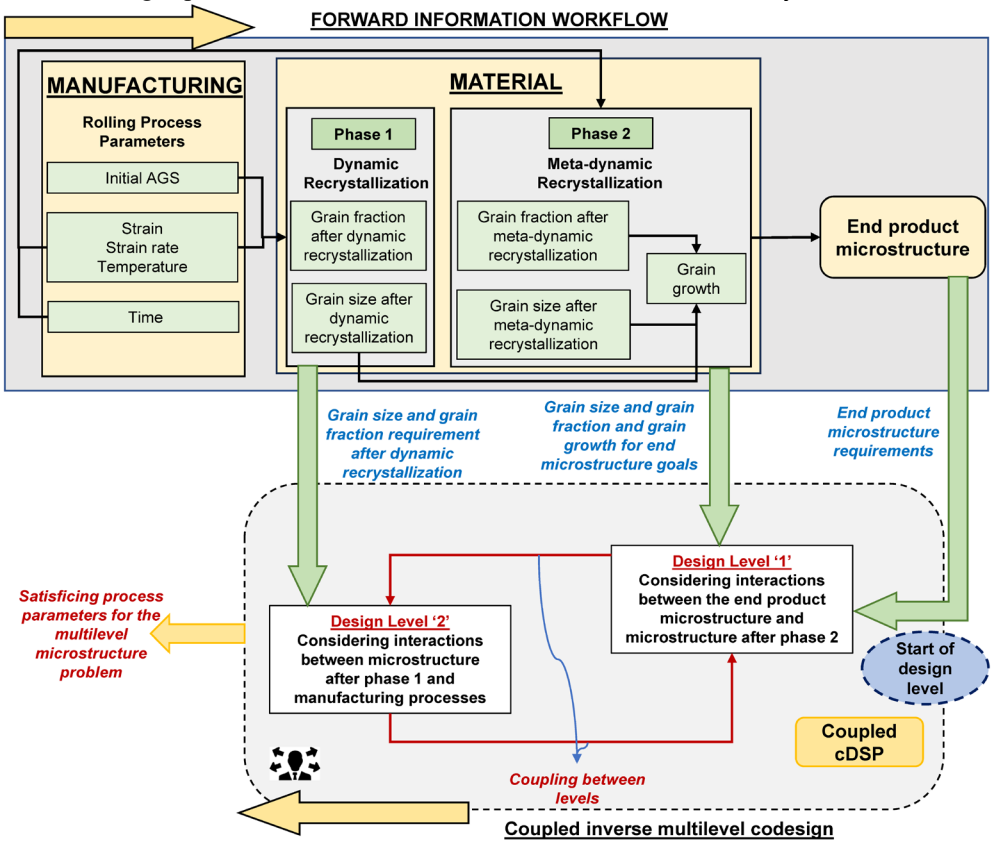


**FIGURE 5:** Multilevel co-design problem for hot rod rolling considering the couplings between the material microstructure and manufacturing processes

In metadynamic recrystallization, the strain rate ($\dot{\varepsilon}_{md}$) and temperature ($T_{md}$), during the metadynamic phase along with time ($t$) after the billet comes out of the roller, define the metadynamic grain size ($D_{md}$) and grain fraction ($X_{md}$). This phase is followed by grain growth. Information on dynamic grain size ($D_{dyn}$) from the dynamic phase and metadynamic grain size ($D_{md}$) and the grain fraction ($X_{md}$) from the metadynamic phase is used to calculate the grain size after grain growth ($D_{gg}$). The empirical models used to define these relations and their sources are included in the Appendix. We notice in the problem that there exist interrelations between the microstructure phases when viewed as an inverse design problem. The manufacturing process variables influence the microstructure formed at each of the phases, and the final austenite microstructure is determined by the microstructures formed in the preceding phases. Therefore, realizing hot rolled rods with a targeted microstructure requires the collective consideration of the (i) manufacturing processing history, (ii) material microstructure, and (iii) the interactions between them. The co-design exploration of the problem is carried out by formulating a coupled cDSP formulation considering the manufacturing process-material microstructure-product interactions, as shown in Figure 5 (see the coupled cDSP in Figure). Next, we explain the usage of the multilevel decision support framework presented in Section 3 to formulate and explore the co-design problem.

*Block A:* Formulating the design problem by collecting level-specific information.

The design of the two phases of the rolling process starts at Step A1 of the given framework.

*Step A1:* The two microstructural phases of the rolling process are considered as two design levels in this problem. Level 1 involves decisions regarding the formulation of grain size after grain growth and grain size and grain fraction after metadynamic recrystallization. Level 2 involves decisions regarding the dynamic phase of the rolling process, which affects the design of the end microstructure.

*Step A2:* Information specific to design levels 1 and 2 is collected in this step. At design level 1, decisions are made for the design variables identified by strain rate ($\dot{\varepsilon}_{md}$) and temperature ($T_{md}$) for the metadynamic phase and time passed ($t$) after the billet comes out of the roller. The strain rate ($\dot{\varepsilon}_{d}$), and temperature ($T_d$) for the dynamic phase are considered as coupling variables from design level 1. These variables define the microstructure goals after metadynamic recrystallization and grain growth. The microstructure requirements for metadynamic grain size ($D_{md}$), grain fraction ($X_{md}$) and recrystallized grain size after grain growth ($D_{gg}$) defined at design level 1 are to achieve the target values of 14 μm, 0.996, and 20μm, respectively. The empirical models used to establish the relations are provided in Appendix A1.

At design level 2, decisions are made for strain rate ($\dot{\varepsilon}_{dc}$), temperature ($T_{dc}$), strain ($\varepsilon$) during the dynamic recrystallization process, and initial austenite grain size (IAGS) before rolling to achieve the required microstructure at the end of the dynamic recrystallization phase. The microstructure requirements for dynamic grain size ($D_{dync}$) and grain fraction ($X_{dyn}$) defined at design level 2 are to achieve the target values of 11 μm and 0.9, respectively. The empirical models used to establish the relations are provided in Appendix A2.

*Step A3:* Dynamic grain size is a parameter that is used to define the goals in both design levels and hence acts as a coupling variable. The strain rate and temperature design variables during the dynamic recrystallization phase define dynamic grain size and are therefore used as the coupling variables between the levels in our formulation. To maintain consistent dynamic grain size values throughout both design levels, the design variables, strain rate, and temperature must be the same for the dynamic phase in both design levels 1 and 2. Therefore, a consistency constraint is defined for these variables. The consistency constraints ensure that the dynamic phase's temperature and strain rate values are the same in design levels 1 and 2.

*Block B:* Modeling decision support problems across multiple levels and their interactions.

*Step B1:* In this step, a decision support problem is formulated using the information from block A. The decisions of the design level 1 and 2 and their interactions are modeled using the c-cDSP construct. In design level 2, a copy of design variables is used for the two coupling variables - strain rate and temperature. To maintain consistency, two consistency constraints are defined in design level 2 for these design variables. This is used to analyze the interactions between the two levels and is mentioned in the *Satisfy* section of the c-cDSP construct. The target values of the goals for the c-cDSP are defined in Step A2. Constraints are defined in the *Satisfy* section of the c-cDSP construct to account for the manufacturing processing conditions.

The deviation function used in the c-cDSP formulation combines the preemptive and Archimedean formulations. The decisions in the rolling process of the manufacturing systems are made hierarchically, with decisions at level 1 being made before decisions at level 2. This hierarchical relation between the two levels is captured using the preemptive formulation. The priority of the multiple goals at the individual level is modeled using the Archimedean formulation. The preemptive and Archimedean formulation is defined in the *Minimize* section of the c-cDSP construct. Designers use the combination of preemptive and Archimedean formulations to consider many goals at design levels and the relation between design levels 1 and 2 in a coupled decision problem formulation.

The formulated coupled-cDSP (c-cDSP) for the hot rod rolling process considering interactions between design levels 1 and 2 is given below:

***Given***

*(a) Constants*

*(i) Gas Constant,* $R = 8.314\ J/moleK$

*(ii) Activation Energy,* $Q_d = 312000\ J/mole$

*(b) Design variables* $(x_i)$ *and their bound at design level 1*

*(i)* $1250\ K \leq x_1(T_{md}) \leq 1600\ K$

*(ii)* $9.000\ s^{-1} \leq x_2(\dot{\varepsilon}_{md}) \leq 18.000\ s^{-1}$
*(iii)* $0.05\ s \leq x_3(t) \leq 0.100\ s$
*(iii)* $1250\ K \leq x_4(T_d) \leq 1600\ K$
*(iv)* $9.000\ s^{-1} \leq x_5(\dot{\varepsilon}_d) \leq 18.000\ s^{-1}$
*Design variables* $(x_i)$ *and their bound at design level 2*
*(i)* $40\ \mu m \leq x_6(IAGS) \leq 100\ \mu m$
*(ii)* $0.65 \leq x_7(\varepsilon) \leq 1.000$
*(iii)* $1250\ K \leq x_8(T_{dc}) \leq 1600\ K$
*(iv)* $9.000\ s^{-1} \leq x_9(\dot{\varepsilon}_{dc}) \leq 18.000\ s^{-1}$

*(c) End requirements at design level 1*
*(i) Achieve target metadynamic recrystallized grain fraction* $(X_{md}) = 0.996$
*(ii) Achieve target metadynamic grain size* $(D_{md}) = 14\ \mu m$
*(iii) Achieve target value for austenite grain size after grain growth,* $D_{gg} = 20\ \mu m$
*End requirements at design level 2*
*(i) Achieve target dynamic recrystallized grain fraction* $(X_{dyn}) = 0.9$
*(ii) Achieve target dynamic grain size* $(D_{dync}) = 11\ \mu m$

*The models used to find the end requirements at design levels 1 and 2 are provided in the appendix.*
***Find***
*(a) Design Variables:* $x_i$*, where* $i = 1,2,3,4,5,6,7,8,9$
*(b) Deviation Variables:* ${d_k}^+$ *and* ${d_k}^-$*, where* $k = 1,2,3,4,5$
***Satisfy***
*(a) Level 1 Design Constraints:*
*(i)* $1 - X_{md} \geq 0$
*(ii)* $D_{gg} - D_{md} \geq 0$
*(iii)* $AD_{RX} - D_{dyn} \geq 0$

*Level 2 Design Constraints:*
*(i)* $T_d = T_{dc}$
*(ii)* $\dot{\varepsilon}_d = \dot{\varepsilon}_{dc}$
*(iii)* $\varepsilon - \varepsilon_c \geq 0$
*(iv)* $1 - X_d \geq 0$
*(v)* $X_d - 0.7 \geq 0$
*(vi)* $IAGS - D_{dync} \geq 0$
*(vii)* $D_{dync} - 7 \geq 0$
*(b) Level 1 Goals*
*(i) Maximize metadynamic recrystallized grain fraction (G1),*
$\frac{X_{md}(X_i)}{X_{md,Target}} + {d_1}^- - {d_1}^+ = 1$
*(ii) Minimize metadynamic recrystallized grain size (G2),*
$\frac{D_{md,,Target}}{D_{md}(X_i)} - {d_2}^- + {d_2}^+ = 1$
*(iii) Maximize value for austenite grain size after grain growth (G3),*
$\frac{D_{gg}(X_i)}{D_{gg,Target}} + {d_3}^- - {d_3}^+ = 1$
*Level 2 Goals*
*(i) Maximize dynamic recrystallized grain fraction (G4),*
$\frac{X_{dyn}(X_i)}{X_{dyn,Target}} + {d_4}^- - {d_5}^+ = 1$
*(ii) Minimize metadynamic recrystallized grain size (G5),*
$\frac{D_{dync,Target}}{D_{dync,}(X_i)} - {d_5}^- + {d_5}^+ = 1$

*(b) Variable bounds at Design Level 1*
*(i)* $1250\ K \leq T_{md} \leq 1600\ K$
*(ii)* $9.000\ s^{-1} \leq \dot{\varepsilon}_{md} \leq 18.000\ s^{-1}$
*(iii)* $0.05\ s \leq t \leq 0.100\ s$
*(iii)* $1250\ K \leq T_d \leq 1600\ K$
*(iv)* $9.000\ s^{-1} \leq \dot{\varepsilon}_d \leq 18.000\ s^{-1}$
*Variable bounds at Design Level 2*
*(i)* $40\ \mu m \leq IAGS \leq 100\ \mu m$
*(ii)* $0.65 \leq \varepsilon \leq 1.000$
*(iii)* $1250\ K \leq T_{dc} \leq 1600\ K$
*(iv)* $9.000\ s^{-1} \leq \dot{\varepsilon}_{dc} \leq 18.000\ s^{-1}$

*Deviation variable bounds*
${d_k}^+, {d_k}^- >= 0$ *and* ${d_k}^+ * {d_k}^- = 0$
***Minimize***
*Preemptive formulation at two levels*
*The deviation function Z needs to be minimized.*
*Min* $Z = (f_1, f_2)$
*Priority 1: Design Level 1 (Archimedean Formulation)*

$$f_1 = \sum W_k({d_k}^+ + {d_k}^-)$$

*where* $W_k$ *= weight assigned to the deviations of the individual goals from the target values,* $\sum W_k = 1$ *and* $k = 1,2,3$
*Priority 2: Design Level 2 (Archimedean Formulation)*

$$f_2 = \sum W_k({d_k}^+ + {d_k}^-)$$

*where* $W_k$ *= weight assigned to the deviations of the individual goals from the target values,* $\sum W_k = 1$ *and* $k = 4,5$.

*Block C: Gene*ration of design scenarios across levels 1 and 2.

The c-cDSP construct is executed using the DSIDES platform for different design scenarios created considering design levels 1 and 2.

*Step C1:* We formulate different design scenarios for the multilevel problem in this step. All possible combinations of design scenarios at level 1 and level 2 are considered to create a multilevel design scenario. Latin hypercube sampling (LHS) design is used to create weight scenarios for individual levels by assigning different weight combinations for goals at each level. LHS design is used to effectively cover the multilevel design space. We considered 13 LHS design scenarios at each level, creating 169 multilevel design scenarios. Six more scenarios with full weight to one goal and zero to the others for individual level are also considered to capture the extreme ends of the design scenarios. We have 175 design scenarios with different weight preferences assigned to the individual goals within and between the levels. We list selected design scenarios in Table 1.

**TABLE 1.** Sample multilevel design scenario

| Design Scenario # | Design Level 1 Weights | | | $\sum W_i$ | Design Level 2 Weights | | $\sum W_i$ |
|---|---|---|---|---|---|---|---|
| | $W_1$ | $W_2$ | $W_3$ | | $W_4$ | $W_5$ | |
| 1 | 0.33 | 0.13 | 0.54 | 1 | 0.61 | 0.39 | 1 |
| 2 | 0.33 | 0.13 | 0.54 | 1 | 0.5 | 0.5 | 1 |
| - | - | - | - | - | - | - | - |
| 71 | 0.26 | 0.68 | 0.06 | 1 | 0.17 | 0.83 | 1 |
| 72 | 0.26 | 0.68 | 0.06 | 1 | 0.26 | 0.74 | 1 |
| - | - | - | - | - | - | - | - |
| 174 | 0 | 0 | 1 | 1 | 1 | 0 | 1 |
| 175 | 0 | 0 | 1 | 1 | 0 | 1 | 1 |

*Step C2:* We execute the c-cDSP using the DSIDES platform for each of the 175 multilevel design scenarios to generate solutions for the goals across design levels 1 and 2.

*Block D:* Visualization and simultaneous co-design exploration of the multilevel solution space.

The solution space generated in block C is further visualized and explored in this block using the following steps.

*Step D1:* We begin this step by training the iSOM algorithm. iSOM supports the simultaneous visualization of multilevel design spaces. We train the algorithm using the different weight scenarios across the two levels as input and the corresponding goal values as output. The trained iSOM provides a 2-dimensional visualization of the design and solution spaces, namely the five input plots of the input goal weights and five output plots of the achieved goal values in design levels 1 and 2. The iSOM plots are shown in Figure 6. On the top are the input weights, followed by the corresponding goals. The red dots in the hexagonal grid of the goal plots indicate the design scenarios mapped to the specific grid.

*Step D2*: The co-design exploration is carried out using the iSOM plots. The iSOM plots allow the designer to study the interrelations between the input and output plots and also the relations between the output plots. This helps carry out simultaneous co-design exploration of the solution space and find common satisficing solution regions that satisfy and suffice the requirements of the designers at both levels. The co-design exploration begins with assigning a satisficing limit for all the goals to identify a common satisficing solution. The designer/s needs to use their domain expertise to define satisficing limits for the goals.

The initial satisficing limit for the goals for design levels 1 and 2 are identified as shown in Table 2 below.

**TABLE 2.** Initial satisficing limits for the multilevel goals

| Level 1 | Level 2 |
|---|---|
| Goal 1, G1 ($X_{md}$) ≥ 0.996 | Goal 4, G4 ($X_{dyn}$) ≥ 0.9 |
| Goal 2, G2 ($D_{md}$) ≤ 14 µm | Goal 5, G5 ($D_{dync}$) ≤ 11 µm |
| Goal 3, G3 ($D_{gg}$) ≥ 20 µm | |

The red-bordered hexagonal grids in Figure 6 are the satisficing solution region for individual goals for the assigned initial limit. Next, we discuss the steps involved in the systematic co-design exploration of the solution spaces to identify satisficing solutions.

*Step 1*: Designers explore the iSOM plots and checks if there are grids that are common for all the goals in design levels 1 and 2. On analyzing Figure 6, we see that there are no common grids that satisfy the requirements for all five goals across design levels 1 and 2. In such a scenario, the designer moves to Step 2 to identify satisficing solutions.

*Step 2:* In this step, we propose one strategy that designers can use to systematically identify satisficing solutions. Since there is no common satisficing solution region, the designer needs to first identify critical goal/s that cannot be relaxed as per design requirements. The designer needs to use their judgment and domain knowledge to carry out this process.

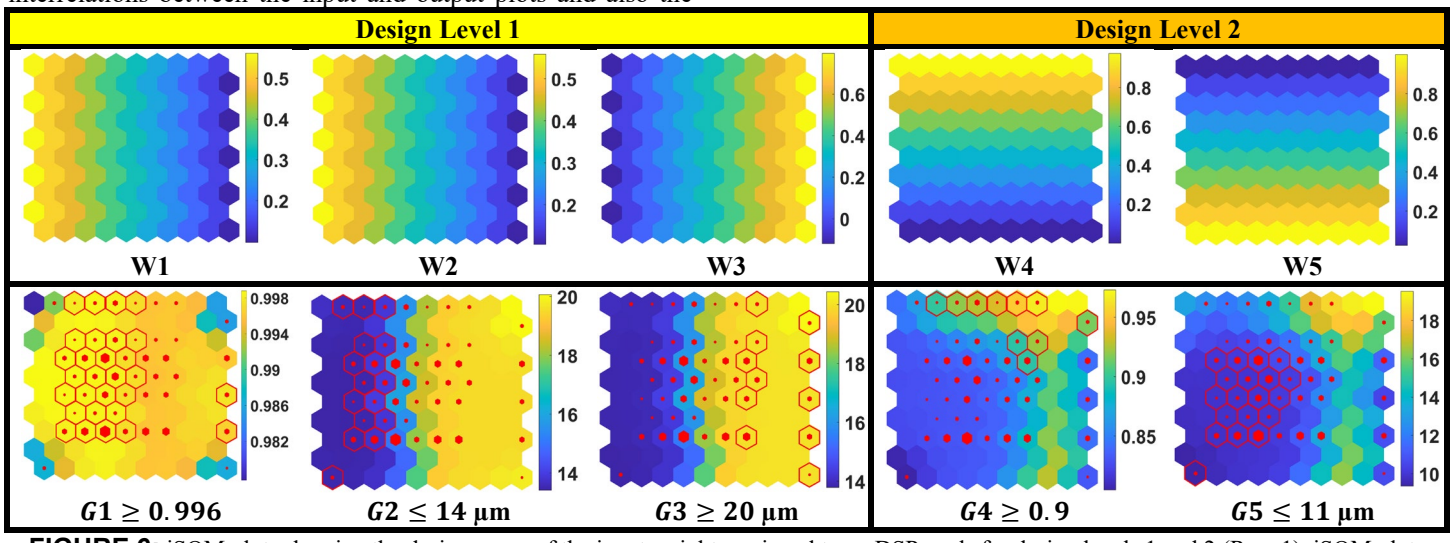


**FIGURE 6:** iSOM plots showing the design space of the input weights assigned to c-cDSP goals for design levels 1 and 2 (Row 1). iSOM plots showing the achieved values of goals in design levels 1 and 2 (Row 2). The hexagonal iSOM grid points highlighted in red indicate satisficing solution regions for the individual goals. The red dots indicate design scenarios mapped to the iSOM grid points. The yellow region indicates a higher value, and the blue region indicates a lower value in the plots.

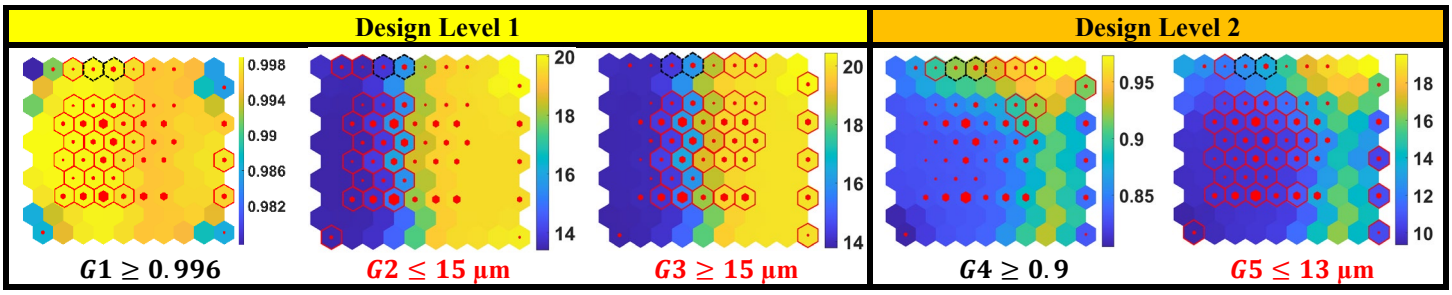


**FIGURE 7:** iSOM plots for all goals across design levels 1 and 2 with the updated satisficing goal limits. The hexagonal iSOM grid points highlighted in red indicate satisficing solution regions for the individual goals with new satisficing limits. The red dots indicate design scenarios mapped to the iSOM grid points. The common satisficing solutions across design levels 1 and 2 are highlighted using a black dashed border.

**TABLE 3.** Achieved goal values in the common iSOM grid points for design levels 1 and 2.

| Design Scenario | W1 | W2 | W3 | W4 | W5 | G1 | G2 (µm) | G3 (µm) | G4 | G5 (µm) |
|---|---|---|---|---|---|---|---|---|---|---|
| 22 | 0.34 | 0.42 | 0.24 | 0.95 | 0.05 | 0.99911 | 13.4111 | 13.8728 | 0.92753 | 13.44868 |
| 48 | 0.52 | 0.24 | 0.24 | 0.95 | 0.05 | 0.99761 | 19.4925 | 20.0061 | 0.98319 | 19.48021 |
| 87 | 0.21 | 0.58 | 0.21 | 0.95 | 0.05 | 0.99911 | 13.4111 | 13.8728 | 0.92753 | 13.44868 |
| 100 | 0.44 | 0.44 | 0.12 | 0.95 | 0.05 | 0.99905 | 13.4122 | 13.8645 | 0.82838 | 9.894979 |
| 113 | 0.74 | 0.1 | 0.16 | 0.95 | 0.05 | 0.99761 | 19.4922 | 20.0061 | 0.98320 | 19.46283 |
| 152 | 0.49 | 0.29 | 0.22 | 0.95 | 0.05 | 0.99910 | 13.4146 | 13.8762 | 0.92608 | 13.43289 |

**TABLE 4.** Design variable values corresponding to the common satisficing solutions/design scenarios

| Design Scenario | Design Level 1 | | | | | Design Level 2 | | | |
|---|---|---|---|---|---|---|---|---|---|
| | $T_{md}$ (K) | $\dot{\varepsilon}_{md}$ ($s^{-1}$) | $t$ (s) | $T_d$ (K) | $\dot{\varepsilon}_d$ ($s^{-1}$) | $IAGS$ (µm) | $\varepsilon$ | $T_{dc}$ (K) | $\dot{\varepsilon}_{dc}$ ($s^{-1}$) |
| 22 | 1250 | 17.9999 | 0.099951 | 1313.95 | 9.2857 | 40.0005 | 0.993005 | 1313.95 | 9.2857 |
| 87 | 1250 | 17.9999 | 0.099951 | 1313.95 | 9.2857 | 40.0005 | 0.993005 | 1313.95 | 9.2857 |
| 100 | 1250.01 | 17.9987 | 0.099213 | 1254.33 | 9.07117 | 40.0073 | 0.990322 | 1254.33 | 9.07117 |
| 152 | 1250 | 17.9798 | 0.099994 | 1313.19 | 9.18023 | 40.0005 | 0.989808 | 1313.19 | 9.18023 |

In this problem, G4, the dynamic recrystallization grain fraction goal is a critical goal. To obtain a suitable dynamically recrystallized microstructure, it is essential to maximize the grain fraction. Therefore, the requirement for G4 has to be always greater than 0.9. Hence, G4 is kept fixed, and the rest, namely, G1, G2, G3, and G5, are selected as goals where the designer can make relaxations or design adjustments.

*Step 3:* In this step, the designer analyzes the goals identified individually and relaxes their satisficing limits in order to identify a common satisficing region. Let us consider the scenario where the designer picks goal G5. There is no common satisficing grid between G4 and G5. The designer must relax the goal to find at least one common grid point for both goals. However, the designer must also focus on not relaxing the goal beyond an allowable limit to find the common grid points. In this case, we relax the goal G5 target from 11 µm to 13 µm. This results in a few common gird points for both G4 and G5. Now, let us say the designer looks into G1. G1 has common grid points with G4. Therefore, there is no need to relax the goal G1 as satisficing grids are found. Let us consider goals G2 and G3 next. We notice from Figure 6 that the values for both these goals are very similar. However, the target regions of interest in these two goals are conflicting. The conflicting behavior for both these goals leads the satisficing solution region to be in opposite directions. The red-bordered hexagon in the iSOM plots of Figure 6 for G2 and G3 marks the satisficing limit for both goals. Therefore, to find a common region, there is a need to relax both goals G2 and G3 so that the relaxation does not adversely impact both goals and simultaneously identifies a common region for goals G4, relaxed G5, and G1. We notice that when the target values of G2 and G3 are relaxed to 15 µm, we are able to identify two common satisficing grid points for all five design goals across design levels 1 and 2.

With the updated satisficing limits, we see in Figure 7 that all five goals have two common satisficing grids, marked with a black dotted line. These two grid points are the common satisficing solutions for all five goals across design levels 1 and 2. Six design scenarios are mapped to these common iSOM grid points. The goal values associated with the identified common grid points are presented in Table 3.

After analyzing the results presented in Table 3, we identify four design scenarios (22, 87, 100, 152; grey shaded in Table 3) as common satisficing solutions. Design scenarios 48 and 113, from Table 3, have a G2 ($D_{md}$) value of 19.49 µm, G5 ($D_{dyn}$) value of 19.46 µm. These values exceed the updated satisficing limits. Hence, we are excluding these two design scenarios from the list of common satisficing solutions.

On analyzing the goal values for design level 1, we see that the four common satisficing design scenarios (22, 87, 100, 152: grey shaded in Table 3) achieve very similar values. The goals of design level 1, metadynamic grain fraction, $X_{md}$ (G1), metadynamic grain size, $D_{md}$ (G2), and grain size after grain

growth, $D_{gg}$ (G3) achieves the goal values of 0.999, 13.41 μm and 13.87 μm, respectively. At design level 2, for three of these four design scenarios (22, 87, and 152), the dynamic grain fraction, $X_{dyn}$ (G4) has a value of 0.92, and the corresponding dynamic grain size, $D_{dync}$ (G5) has a value of 13.44 μm. The remaining common design scenario (100) has a G4 value of 0.82 and a G5 value of 9.89 μm. The design variable values corresponding to these four common satisficing solutions are provided in Table 4.

The design variables required to achieve the goals in design level 1, namely temperature ($T_{md}$), strain rate ($\dot{\varepsilon}_{md}$) and the time interval ($t$), for metadynamic and grain growth goals remain similar for all design scenarios with values around 1250 K, 17.99 $s^{-1}$, and 0.0999 s, respectively. At design level 2, two of the design variables, namely, initial austenite grain size ($IAGS$) and strain ($\varepsilon$), achieve similar values across all four design scenarios with values of 40 μm and 0.99, respectively. Design scenarios 22, 87, and 152 achieve temperature ($T_{dc}$) and strain rate ($\dot{\varepsilon}_{dc}$) values of 1313.95 K and 9.2 $s^{-1}$, respectively. These values result in achieving goal targets for goals G4 and G5 (values of 0.92 and 13.44 μm, respectively). Design scenario 100 achieves temperature ($T_{dc}$) and strain rate ($\dot{\varepsilon}_{dc}$) values of 1254.33 K and 9.07 $s^{-1}$, respectively. These values result in achieving an improved value for goal G5 (value of 9.89 μm) in design scenario 100. At the same time, we see that the achieved value for goal G4 drops down to 0.82 for this design scenario compared to the other three scenarios. Due to the consistency constraint between design level 1 and design level 2 regarding the temperature and strain rate for dynamic recrystallization, the values for these two variables remain unchanged and consistent across both design levels. Based on the analysis of Table 4, designers are able to understand the effect of design variables on the design goals. After analyzing the results for design levels 1 and 2, we see that choosing any design scenario from the four satisficing design scenarios will meet the goal requirements for level 1. However, for design level 2, we can choose either design scenario 100 for an improved dynamic recrystallized grain size goal (G5) or choose any of the other three design scenarios (22, 87, or 152) for improved dynamic recrystallized grain fraction goal (G4). The selection of these design scenarios will be based on the designers' preference for the problem.

Using the iSOM plots shown in Figures 6 and 7, designers are able to understand the relationships among the goals within and between the multiple levels. In the plots, the color bar exhibits a gradual transition from blue to yellow, where blue indicates low values and yellow indicates high values. For example, at design level 1 $D_{md}$ (G2) and $D_{gg}$ (G3) goals exhibit similar behavior as depicted in both iSOM plots for G2 and G3. Hence, focusing on achieving a lower G2 value will also result in a lower G3 value. Similarly, at design level 2, a similar pattern is seen in the iSOM plots associated with G4 and G5. Therefore, focusing on achieving lower G5 values will also result in lower G4 values. This allows the designer to easily interpret any design conflicts between the goals and make appropriate design trade-offs. Moreover, the designer is also able to understand and analyze the relationships between the input weights assigned to the goals in the c-cDSP and the corresponding achieved values of the goals and also the effects of the assigned weights on the other goals using the iSOM plots. From Figure 6, a higher value in the weight for goal 2, indicated by the yellow region in W2, results in a lower value for that goal, as shown by the blue region for goal G2. This shows that the designer's requirement to minimize goal 2 is captured appropriately in the iSOM plots, as a higher value of the input weight results in a lower value for the goal.

The proposed framework, thus, supports designers in modeling the multilevel design problem and performing simultaneous co-design exploration to identify satisficing design solutions. The framework supports understanding (i) the relationships between the goals within and between levels, and (ii)identifying satisficing regions of interest given the multilevel interactions, couplings, and multidisciplinary designers.

## 5. CLOSING REMARKS

In this paper, we present a co-design exploration framework for multilevel decision support. The framework involves the integration of two design constructs, namely the coupled compromise Decision Support Problem (c-cDSP) and a machine learning-based visualization tool called interpretable Self Organizing Map (iSOM). Using the framework, designers are able to (i) model a multilevel design problem with conflicting goals at individual levels and interactions between levels as a coupled compromise decision support problem, and (ii) simultaneously explore the multilevel solution spaces to identify common sets of satisficing design solutions that support co-design.

The key functionalities of the framework that we present in this paper include:

(a) facilitating the formulation of the multilevel design problems with many conflicting goals at individual levels and interactions and couplings between the levels. The functionality is achieved using consistency constraints and combining the preemptive and Archimedean formulations in the c-cDSP. The use of consistency constraints between the levels helps to capture the interactions and couplings between the levels by keeping a common set of design variables constant for both levels. By combining the preemptive and Archimedean formulation in the formulated c-cDSP, the designers are able to connect the multiple levels and account for the conflicting goals in each level into a coupled decision support problem.

(b) facilitating the visualization and co-design exploration of multilevel design spaces. The functionality is achieved with the help of the interpretable self-organizing map (iSOM) construct. iSOM offers the capability of simultaneous solution space visualization of the design scenarios formulated using c-cDSP by generating two-dimensional plots for all the goals. Efficient co-design exploration is realized using the iSOM tool to visualize and explore the multilevel design spaces simultaneously. Co-design exploration has an advantage over other multilevel design exploration approaches based on

 

sequential design as it supports the management of design conflict and ensures system performance.

We test the efficacy of the framework using the hot rod rolling problem, focusing on the interactions between the dynamic and metadynamic phases of material recrystallization and the thermo-mechanical processing during the hot rolling process. The framework is generic and supports the co-design exploration of systems characterized by multilevel interactions, couplings, and multidisciplinary designers.


## ACKNOWLEDGEMENTS

This material is based upon work supported by the National Science Foundation under Grant No. 2301808.


## APPENDIX A: Mathematical models for hot rolling of steel rods

### A1. Models used in Design Level 1.

- Zenner Holloman Parameter metadynamic [43],

$$Z_{md} = \dot{\varepsilon}_{md} exp\left(\frac{Q_d}{R \times T_{md}}\right)$$

- Time for 50% recrystallization after metadynamic [43],

$$t_{0.5} = 1.12\, {Z_{md}}^{-0.8} exp\left(\frac{230000}{RT_{md}}\right)$$

- Volume fraction of meta dynamic recrystallized material [43],

$$X_{md} = 1 - exp\left[-0.693\left(\frac{t}{t_{0.5}}\right)^{1.3}\right]$$

- Grain Size after meta dynamic recrystallization [43],

$$D_{md} = (2.6 \times 10^4) Z^{-0.23}$$

- Zenner Holloman Parameter metadynamic [43],

$$Z_d = \dot{\varepsilon}_d exp\left(\frac{Q_d}{R \times T_d}\right)$$

- Grain Size after dynamic recrystallization [43],

$$D_{dyn} = (1.6 \times 10^4) {Z_d}^{-0.23}$$

- Average grain size after Dynamic and Metadynamic Recrystallization [43],

$$AD_{RX} = D_{dyn} + (D_{md} - D_{dyn})\, X_{md}$$

- Grain Growth [44],

$${D_{gg}}^2 = {AD_{RX}}^2 + 1.2 \times 10^7 \times (t - 2.65 t_{0.5}) \exp\left(\frac{-113000}{RT}\right) \text{ if } t < 1$$

### A2. Models used in Design Level 2.

- Critical Strain to decide whether dynamic recrystallization will take place or not [43],

$$\varepsilon_c = (4 \times 10^{-4})(IAGS)^{0.5} {Z_{dc}}^{0.15}$$

- Zenner Holloman Parameter [43],

$$Z_{dc} = \dot{\varepsilon}_{dc}\, exp\left(\frac{Q_d}{R \times T_{dc}}\right)$$

- Volume fraction of recrystallized material [43],

$$X_{dyn} = 1 - exp\left[-0.8\left(\frac{\varepsilon - \varepsilon_c}{\varepsilon_p}\right)^{1.4}\right]$$

- Peak Strain [43],

$$\varepsilon_p = 1.23\varepsilon_c$$

- Grain Size after dynamic recrystallization [43],

$$D_{dync} = (1.6 \times 10^4) {Z_{dc}}^{-0.23}$$

We use $\dot{\varepsilon}_{dc}, T_{dc}, Z_{dc}, D_{dync}$ as copies of the values calculated in design level 1 to ensure consistency.

## REFERENCES


1. Sobieszczanski-Sobieski, J., Agte, J., and Sandusky, J. R., 1998, "Bi-level Integrated System Synthesis (BLISS)," *7th AIAA/USAF/NASA/ISSMO Symposium on Multidisciplinary Analysis and Optimization*, American Institute of Aeronautics and Astronautics, Paper No. AIAA-98-4916.
2. Sobieszczanski-Sobieski, J., and Kodiyalam, S., 2001, "BLISS: A New Method for Two-Level Structural Optimization," *Structural and Multidisciplinary Optimization*, vol. 21, no. 1, pp. 1-13.
3. Kroo, I., Altus, S., Braun, R., Gage, P., and Sobieski, I., 1994, "Multidisciplinary Optimization Methods for Aircraft Preliminary Design," *5th Symposium on Multidisciplinary Analysis and Optimization*, American Institute of Aeronautics and Astronautics, Paper No. AIAA-94-4325-CP.
4. Wang, P., Bai, Y., Fu, C., and Lin, C., 2023, "Lightweight Design of an Electric Bus Body Structure with Analytical Target Cascading," *Frontiers of Mechanical Engineering*, vol. 18, no. 1, pp. 2.
5. Shahan, D. W., and Seepersad, C. C., 2012, "Bayesian Network Classifiers for Set-Based Collaborative Design," *Journal of Mechanical Design*, vol. 134, no. 7, pp. 071001.
6. Arróyave, R., and McDowell, D. L., 2019, "Systems Approaches to Materials Design: Past, Present, and Future," *Annual Review of Materials Research*, vol. 49, no. 1, pp. 103-126.
7. Olson, G. B., 1997, "Computational Design of Hierarchically Structured Materials," *Science*, vol. 277, no. 5330, pp. 1237-1242.
8. McDowell, D., 2018, "Microstructure-Sensitive Computational Structure-Property Relations in Materials Design," In: Computational materials system design. Springer International Publishing, pp 1-25.
9. Simpson, T., Toropov, V., Balabanov, V., and Viana, F., 2008, "Design and Analysis of Computer Experiments in Multidisciplinary Design Optimization: A Review of How Far We Have Come - Or Not," *12th AIAA/ISSMO Multidisciplinary Analysis and Optimization Conference, MAO*, Paper No. AIAA-2008-5802.
10. Simon, H. A., 1956, "Rational choice and the structure of the environment," *Psychological Review*, vol. 63, no. 2, pp. 129-138.
11. Allen, J. K., Panchal, J., Mistree, F., Singh, A., and Gautham, B., 2015, "Uncertainty Management in the Integrated Realization of Materials and Components," *Proceedings of the 3rd World Congress on Integrated Computational Materials Engineering (ICME 2015)*, Vol. 35,pp. 339-346.
12. McDowell, D. L., Panchal, J., Choi, H.-J., Seepersad, C., Allen, J. K., and Mistree, F., 2009, "Integrated Design of Multiscale, Multifunctional Materials and Products," Butterworth-Heinemann.
13. Mistree, F., Smith, W., Bras, B., Allen, J., and Muster, D., 1990, "Decision-Based Design: A Contemporary Paradigm for Ship Design," *Transactions - Society of Naval Architects and Marine Engineers*,vol. 98, pp. 565-597.
14. Mistree, F., Allen, J. K., Woodruff, G. W., and Simon, H., "Position Paper Optimization In Decision-Based Design," *Optimization in Industry*, Palm Coast, FL.

15. Muster, D., and Mistree, F., 1988, "The Decision Support Problem Technique in Engineering Design," *The International Journal of Applied Engineering Education*, vol. 4, no.1, pp. 23-33.
16. Simon, H. A., 1997, Administrative Behavior: A Study of Decision-Making Processes in Administrative Organizations, Free Press, New York.
17. Mistree, F., Hughes, O., and Bras, B., 1993, "The Compromise Decision Support Problem and the Adaptive Linear Programming Algorithm," *Progress in Astronautics and Aeronautics*, vol. 150, pp. 251-251.
18. Adams, B.L., Fullwood, D.T. and Kalidindi, S., 2013, "Microstructure Sensitive Design for Performance Optimization," Elsevier.
19. Kalidindi, S., Niezgoda, S., Landi, G., Vachhani, S., and Fast, T., 2010, "A Novel Framework for Building Materials Knowledge Systems," *Computers Materials & Continua*, vol. 17, no. 2, pp. 103-125.
20. Kalidindi, S., Niezgoda, S., and Salem, A., 2011, "Microstructure Informatics Using Higher-Order Statistics and Efficient Data-Mining Protocols," *JOM: the journal of the Minerals, Metals & Materials Society*, vol. 63, pp. 34-41.
21. Ghosh, S., Anantha Padmanabha, G., Peng, C., Andreoli, V., Atkinson, S., Pandita, P., Vandeputte, T., Zabaras, N., and Wang, L., 2021, "Inverse Aerodynamic Design of Gas Turbine Blades Using Probabilistic Machine Learning," *Journal of Mechanical Design*, vol. 144, no. 2, pp.021706.
22. Sui, F., Guo, R., Zhang, Z., Gu, G. X., and Lin, L., 2021, "Deep Reinforcement Learning for Digital Materials Design," *ACS Materials Letters*, vol. 3, no. 10, pp. 1433-1439.
23. Kim, B., Lee, S., and Kim, J., "Inverse Design of Porous Materials Using Artificial Neural Networks," *Science Advances*, vol. 6, no. 1, pp. eaax9324.
24. Chen, C. T., and Gu, G. X., 2020, "Generative Deep Neural Networks for Inverse Materials Design Using Backpropagation and Active Learning," *Advanced science (Weinheim, Baden-Wurttemberg, Germany)*, vol. 7, no. 5, pp. 1902607.
25. Kumar, S., Tan, S., Zheng, L., and Kochmann, D. M., 2020, "Inverse-designed Spinodoid Metamaterials," *npj Computational Materials*, vol. 6, no. 1, pp. 73.
26. Hou, L., and Jiao, R., 2020, "Data-Informed Inverse Design by Product Usage Information: A Review, Framework and Outlook," *Journal of Intelligent Manufacturing*, vol. 31, pp.529-552.
27. Flores Ituarte, I., Panicker, S., Nagarajan, H. P. N., Coatanea, E., and Rosen, D. W., 2023, "Optimisation-Driven Design to Explore and Exploit The Process–Structure–Property–Performance Linkages in Digital Manufacturing," *Journal of Intelligent Manufacturing*, vol. 34, no.1, pp. 219-241.
28. Martins, J. R. R. A., and Lambe, A. B., 2013, "Multidisciplinary Design Optimization: A Survey of Architectures," *AIAA Journal*, vol. 51, no.9, pp. 2049-2075.
29. Wang, G., and Shan, S., 2007, "Review of Metamodeling Techniques in Support of Engineering Design Optimization," *Journal of Mechanical Design*, vol. 129, no. 4, pp. 370-380.
30. Choi, H., McDowell, D. L., Allen, J. K., Rosen, D., and Mistree, F., 2008, "An Inductive Design Exploration Method for Robust Multiscale Materials Design," *Journal of Mechanical Design*, vol. 130, no. 3, pp. 031402.
31. Nellippallil, A. B., Mohan, P., Allen, J., and Mistree, F., 2020, "An Inverse, Decision-Based Design Method for Robust Concept Exploration," *Journal of Mechanical Design*, vol. 142, no. 8, pp. 081703.
32. Nellippallil, A. B., Rangaraj, V., Gautham, B., Singh, A., Allen, J., and Mistree, F., 2018, "An Inverse, Decision-Based Design Method for Integrated Design Exploration of Materials, Products and Manufacturing Processes," *Journal of Mechanical Design*, vol. 140, n0. 11, pp. 111403.
33. Sharma, G., Allen, J.K., and Mistree, F., 2021, "A Method for Robust Design in A Coupled Decision Environment," *Design Science*, vol. 7, e. 23.
34. Sharma, G., Allen, J. K., and Mistree, F., 2023, "Exploring Robust Decisions in the Design of Coupled Engineered Systems," *Journal of Mechanical Design*, vol. 145, no. 12, pp. 121402.
35. Baby, M., and Nellippallil, A. B., 2024, "An Information-Decision Framework for the Multilevel Co-Design of Products, Materials, and Manufacturing Processes," *Advanced Engineering Informatics*, vol. 59, pp.102271.
36. Baby, M., Rama Sushil, R., Ramu, P., Allen, J. K., Mistree, F., and Nellippallil, A. B., 2023, "Robust, Co-design Exploration of Multilevel Product, Material, and Manufacturing Process Systems," *Integrating Materials and Manufacturing Innovation*, pp. 1-22.
37. Sushil, R. R., Baby, M., Sharma, G., Nellippallil, A. B., and , and Ramu, P., 2022, , 2022, "Data Driven Integrated Design Space Exploration Using ISOM,"*ASME Design Automation Conference*, Paper Number: IDETC2022- 89895.
38. Lenard, J., Cser, L., and Pietrzyk, M., 1999, "Mathematical and Physical Simulation of the Properties of Hot Rolled Products," Elsevier.
39. Hodgson, P. D., and Gibbs, R. K., 1992, "A Mathematical Model to Predict the Mechanical Properties of Hot Rolled C-Mn and Microalloyed Steels," *ISIJ International*, vol. 32,no. 12, pp. 1329-1338.
40. Thole, S., and Ramu, P., 2020, "Design Space Exploration and Optimization Using Self-Organizing Maps," *Structural and Multidisciplinary Optimization*, vol. 62, no. 3, pp. 1071-1088.
41. Richardson, T., Kannan, H., Bloebaum, C., and Winer, E., 2014, "Incorporating Value-Driven Design into the Visualization of Design Spaces Using Contextual Self-Organizing Maps: A Case Study of Satellite Design," *15th AIAA/ISSMO Multidisciplinary Analysis and Optimization Conference*,pp. 2728. 2014.
42. Kohonen, T., and Somervuo, P., 1998, "Self-organizing Maps of Symbol Strings," *Neurocomputing*, Vol. 21, No.1, pp. 19-30.
43. Kuziak, R., Cheng, Y.-W., Glowacki, M., and Pietrzyk, M., 1997, "Modeling of the Microstructure and Mechanical Properties of Steels during Thermomechanical Processing," *NIST Technical Note (USA)*, vol. 1393, pp. 72.
44. Lee, Y., Choi, S., and Hodgson, P., 2002, "Integrated Model for Thermo-Mechanical Controlled Process in Rod (or Bar) Rolling," *Journal of Materials Processing Technology*, vol. 125-126, pp. 678-688.